

Imperial/TP/95-96/23
 astro-ph/9602040
 Submitted to *PRL*

Satellite design parameters for detecting coherence in the microwave sky

Andreas Albrecht and Benjamin D. Wandelt

Blackett Laboratory, Imperial College, Prince Consort Road London SW7 2BZ U.K.

Abstract

Recently it has been realized that observations of fluctuations in the cosmic microwave background (CMB) can reveal very interesting information about the degree of coherence exhibited by the perturbations at early times. This fact should allow sufficiently detailed observations to clearly differentiate among several competing models of structure formation. We study the mission parameters required for a satellite to address the issue of coherence. Our results emphasize the importance of a small beamwidth, and support the cases for the PSI, FIRE and COBRAS/SAMBA satellite proposals (in increasing order of resolving power). Design parameters for a fourth proposal, MAP, have not been made available.

PACS Numbers : 98.80.Cq, 95.35+d

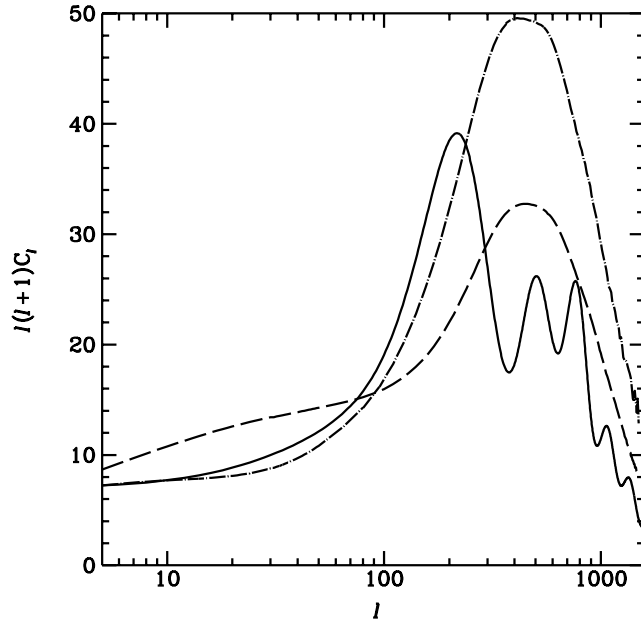


FIG. 1. Angular power spectrum of temperature fluctuations generated by cosmic strings (dashed) and arising from a typical model of scale invariant primordial fluctuations (solid) in arbitrary units. The shape of the string curve for $l \lesssim 100$ (and thus the height of the peak) is very sensitive to existing uncertainties in string networks. This is illustrated by the second string curve (dot-dashed) which represents a second plausible estimate of the spectrum from a cosmic string model. We show only the scalar contribution, in arbitrary units. The string curves are from Fig 4 in [3].

I. INTRODUCTION

Measurements of the Cosmic Microwave Background (CMB) anisotropies have already had a tremendous impact on the field of cosmology. (For a review see [1].) Future measurements promise to greatly increase this impact. New experiments will be measuring the anisotropies with increasing resolution and accuracy, and our theoretical understanding has advanced to the point where tremendous significance can be attached to these new data.

Recently [2,3] it was realized that the degree of coherence in the perturbations at early times will be reflected in striking features in the angular power spectrum. These features should allow observations to clearly differentiate among several competing models of structure formation. As illustrated in Fig 1, the nature of the effect involves the degree to which the so-called “secondary Doppler peaks” are present in the angular power spectrum. It is worth noting that various types of perturbations (including certain “decoherent active” perturbations as discussed in [3] and [4]) can produce secondary peaks. It is the presence or absence of these peaks that concerns us here.

The purpose of this *Letter* is to analyse the design parameters required for a satellite to determine the presence or absence of secondary Doppler peaks. We first describe the fundamental methods and assumptions which are used throughout our discussion. Then we step through a series of pairs of curves. In each pair, one curve has “standard” secondary peaks and one does not. For each pair, we delimit the “design parameter space” which is

able to resolve the differences between the two.

II. METHODS

A. Modelling the satellite

Our methods are the following. We work entirely in “ C_l space”, where the C_l ’s represent the angular power spectrum of microwave anisotropies converted to an angular power spectrum using spherical harmonics in the standard way. On a case-by-case basis we consider pairs of curves C_l which represent key differences one might wish to resolve. The “design parameters” of the experiment are represented by an effective “beam width” θ_{fwhm} and pixel noise T_{pix} which are converted into the expected variance in the C_l for a satellite of given fractional sky coverage f , using an extension of the formula derived in [6]:

$$(\Delta C_l)^2 = \frac{2}{f(2l+1)}(C_l + 4\pi\sigma_{pix}^2 e^{l^2\sigma_b^2})^2 \quad (1)$$

where $\sigma_{pix} = \frac{T_{pix}}{\sqrt{N_{pix}}}$; N_{pix} is the total number of pixels on the cut sky. Each pixel subtends a patch of dimensions $\theta_{fwhm} \times \theta_{fwhm}$. We are assuming a Gaussian beamshape, and hence a beam function of the form $B_l = e^{-l(l+1)\sigma_b}$ [7], where $\sigma_b = \frac{\theta_{fwhm}^2}{2\sqrt{\ln 2}}$. We model limited sky coverage by simply reducing the number of independent modes per l by the constant factor f for all l . This procedure is motivated in [8], where the authors find the naive “guess” $\sigma_{sample}^2 \simeq (1/f)\sigma_{cosmic}^2$ to be essentially correct. We emphasise that we view Eqn 1 as a simple tool for generating realistic variances for the C_l ’s as a function of the parameters θ_{fwhm} , σ_{pix} , and f . How these effective parameters are related to the fundamental design parameters of a given satellite involves understanding specific problems such as the process of foreground subtraction. We do not deal with these issues here.

B. Non-orthogonality of the a_{lm} ’s

Technically, the independent modes a_{lm} which contribute to the C_l ’s are only orthogonal when considering the whole sky. The orthogonal functions for a partial sky (besides being fewer, as already discussed) will tend to get contributions from several a_{lm} ’s. We expect this fact not to invalidate the rough arguments below for the following reasons. Firstly, a major factor in the whole procedure is counting up the right number of independent modes. The factor f in Eqn 1 ensures that we are doing this correctly (at least for large l). Secondly, for reasonably large sky coverage only a handful of nearby l ’s would be mixed to form the true orthogonal functions, and since the C_l ’s (and the error bars) are not too rapidly varying with l , we expect the error bars on the true orthogonal functions to be well estimated by those of the related C_l ’s. Finally, although the first two arguments probably break down for low values of l , the results presented here do not depend crucially on what is happening at low l , so we expect overall not to be making any serious errors.

C. Determining “resolving power”

We are trying to address the question: “Given two theoretical curves $f(l)$ and $g(l)$, which part of parameter space contains the experiments which can confidently distinguish between them?”. To quantify this we calculate the “distance” d between the two curves as

$$d = \sum_{l=2}^{l_{max}} \left(\frac{f - g}{\Delta C_l} \right)^2 \quad (2)$$

using the errors as constructed above. Under the assumption of near-Gaussianity, d will be nearly χ^2 -distributed and we can estimate the confidence p with which the curves can be distinguished for this particular experiment,

$$p = Q\left(\frac{l_{max} - 1}{2}, \frac{d}{2}\right) \quad (3)$$

where Q is the incomplete Gamma Function. We then find a sharp boundary in parameter space between a region of nearly certain distinguishability and a region where experiments fail to distinguish the two curves. These are plotted in the top panels of Figs 2-5. In regions above the heavy curve, there is greater than %99.9 probability of confusing the two curves, and below the curve there is less than %0.1 probability of confusion. Note that the x coordinate in the top panel is noise (in μK) per unit θ_{fwhm} , where θ_{fwhm} (in arc minutes) is the y coordinate. In each of Figs 2-5 the lower panel shows the two curves used, as well as the error bars associate with the point indicated with a \times in the upper panel. (The y axis is in units of μK^2 .)

D. Further Discussion

In this *Letter* we take the view that there are very strong reasons to go for maximum sky coverage. As well as investigating the low l behaviour of the C_l ’s, a single satellite will allow a wide range of scales to be studied. Even though individual ground based experiments can pin down a rather narrow range of smaller angular scales, piecing several such results together into a coherent picture can be tricky, not the least because of the need to get the correct relative normalisation. As we discuss below, the range of possible angular power spectra is quite varied, and we regard the coherent picture which only a satellite can produce to be essential to extracting clear cosmological information from the CMB. For example, in [9] Magueijo and Hobson argue that a long duration low sky coverage interferometry experiment would give a simple way to detect the secondary peaks in Fig 2, but such an experiment would be unable to differentiate the curves in Fig 5¹.

Throughout this *Letter*, we take the sky fraction $f = 0.4$. This seems to be a reasonable “maximum” sky coverage which avoids excessive foreground contamination. As a consequence of large sky coverage, one obtains a large number of independent data points at

¹J. Magueijo, private communication. Magueijo and Hobson also discuss single dish experiments and find results broadly similar to ours.

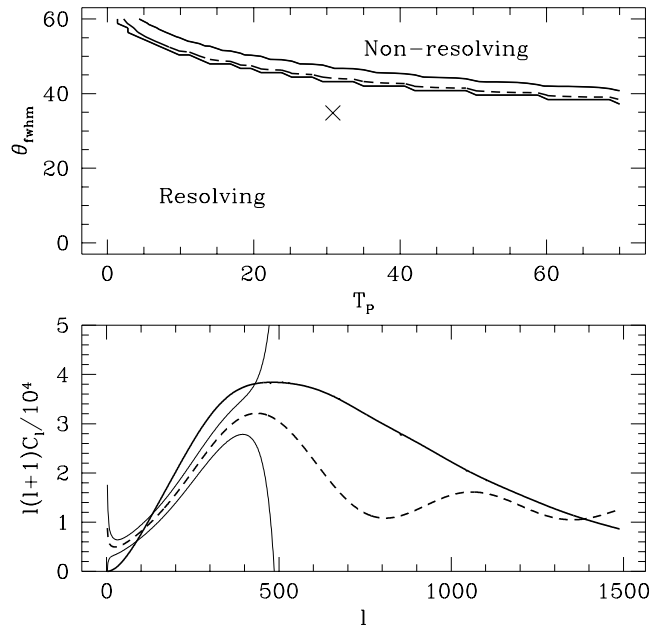


FIG. 2. One of the string curves from Fig 1 paired with an adiabatic (passive) model with $\Omega = 0.3$, $h = 60$, $\Omega_b h^2 = 0.02$ and no tilt (in order to roughly match first peak positions). A wide range of satellites can distinguish between these two curves. The technical details of the plot are provided in Section II

small angular scales. This adds to the ability of the satellite to resolve the secondary peaks, and is the origin of the sharp contrast we find between the “resolving” and “non-resolving regions”.

III. EXPLORING THEORY SPACE

As we have already seen in Fig 1 a given low-coherence theoretical model (such as cosmic strings) may well have an angular power spectrum which differs from “similar” high coherence model on *all* scales. Figure 2 shows the case of two similar curves, one with and one without secondary oscillations. Clearly these curves are sufficiently different to allow a large (but still limited) range of experiments to distinguish between them.

However, we are faced with several theoretical uncertainties which would allow coherent and decoherent model builders to fit the data once it has come in. Cosmic string models are relatively unconstrained at low l . Even after these have been pinned down, there will be a wide range of different types of “decoherent” models based, for example, on different types of cosmic defects. Uncertainties about the details of the inflaton potential will continue to add flexibility to inflationary predictions. Both scenarios are affected by the uncertainties in the values of cosmological parameters such as Ω , Ω_b , h , and Λ , as well as uncertainties in the ionization history. The fact that the primary peak can occur in the same position for defect and inflation models with different Ω generates a further degeneracy. One of the exciting opportunities offered by the coherence issue is that by searching for secondary Doppler peaks one can have an impact on theoretical cosmology which transcends these uncertainties.

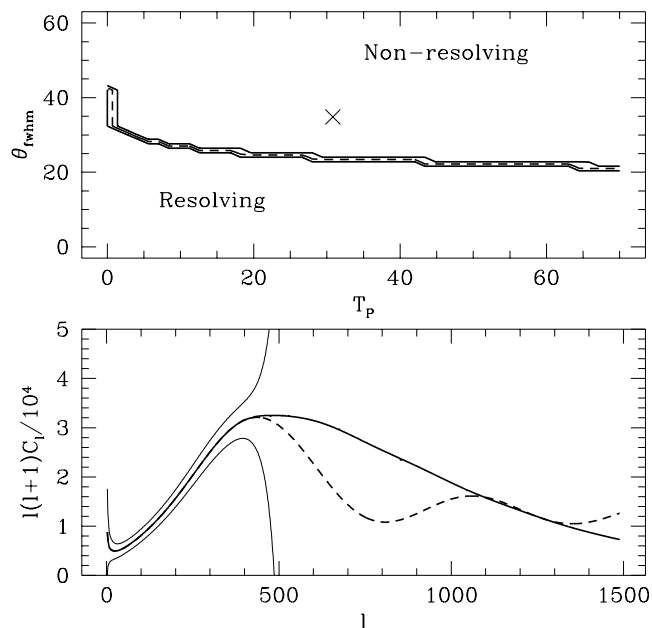


FIG. 3. The two curves from Fig 2 have been forced to match at low l (as one might expect theorists to do if this is where the data lay). Higher resolution experiments are required to pin down the differences, which lie in the secondary Doppler peaks.

In what follows, we step through a series of pairs of curves, each illustrating the kind of pressure that searching for secondary peaks can put on satellite design. In each case, one of the curves has no secondary peaks, and is forced to match the other (oscillating) curve to varying degrees. Many of these curves are constructed “by hand”, rather than being calculated from a particular detailed model. We feel that the prevailing theoretical uncertainties justify this approach. In Fig 3 we have forced the two curves from Fig 2 to match exactly at low l . Much higher resolution experiments are required to resolve the difference between these two curves, since the differences emerge only in the high l region. In Fig 4, we have made a further modification of the curves in Fig 3 so that the curve with no secondary oscillations tracks the inflation curve as much as possible. The useful region in satellite parameter space is reduced even further.

Cosmic string models tend to produce primary peaks at rather small angular scales, so it is not surprising that looking for the secondary oscillations makes high demands on the resolution. Suppose however, that the position of the primary peak is at the larger angular scale indicated in the standard $\Omega = 1$ CDM model. One would still want to search for the presence of secondary peaks, as a test for coherence². Figure 5 shows that even for this case the resolution required to test for secondary oscillations is considerable. Note that the experiment indicated by the \times can easily resolve the primary peak, but is unable to investigate the presence of secondary oscillations.

²A standard CDM primary peak *without* oscillations would be an extremely important result. It has been argued that this situation is very difficult to achieve [3] (see also [5]).

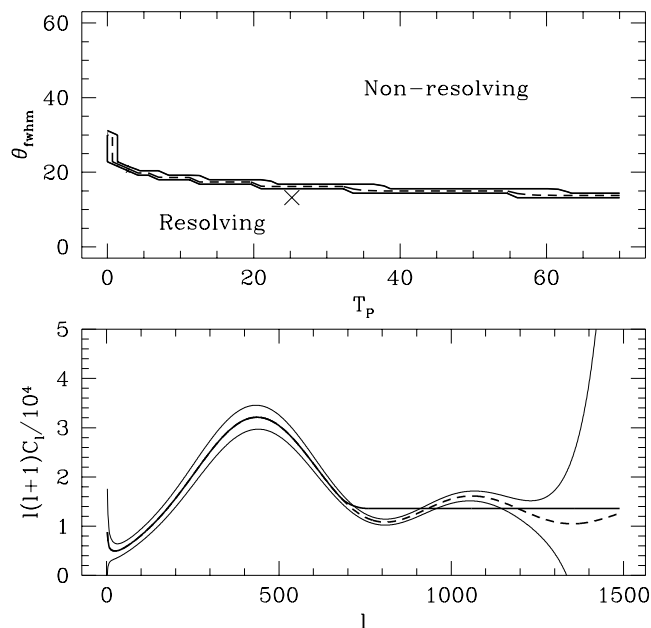


FIG. 4. Further modification of one curve from Fig 3 attempts to maximize the similarity between the two curves without introducing secondary peaks. Even more pressure is placed on the satellite design.

IV. CONCLUSIONS

The search for secondary oscillation in the CMB angular power spectrum holds a deep significance for the field of cosmology. We have argued that a thorough search requires a satellite with sufficient resolution. The main point of this *Letter* is to make sure that such a satellite gets built. There are four satellite proposals presently under consideration and we outline their resolving power here. It is not trivial to translate the realistic error bars (after eg foreground subtraction) into the two parameters used here³. Still, [10] suggests that the “FIRE” satellite can be roughly described by $\theta_{fwhm} = 8'$ and $T_{Pix} = 24.7\mu K$, and PSI by $\theta_{fwhm} = 12.6'$ and $T_{Pix} = 25\mu K$. Of these two, the lower resolution error bars (PSI) appear on Fig 4 (the figure which places the greatest demands on satellite design). We conclude that both of these experiments would be effective in searching for secondary oscillations. (The PSI experiment is actually rather close to the edge of the “resolving” region.) The COBRAS/SAMBA proposal has been analysed in [12]. Even the most pessimistic analysis from [12] implies an even greater resolving power than that of PSI or FIRE. The design parameters for the fourth proposal, MAP [11], are not public information.

The presence or absence of secondary Doppler peaks in the CMB power spectrum is of fundamental interest. Our analysis emphasizes small beamwidth as a crucial design parameter for their detection, and thus strengthens the case for a high resolution CMB

³In order to allow a more systematic discussion, we are making our sets of curves (and other information) available at “<http://euclid.tp.ph.ic.ac.uk/~albrecht/satellites/>”

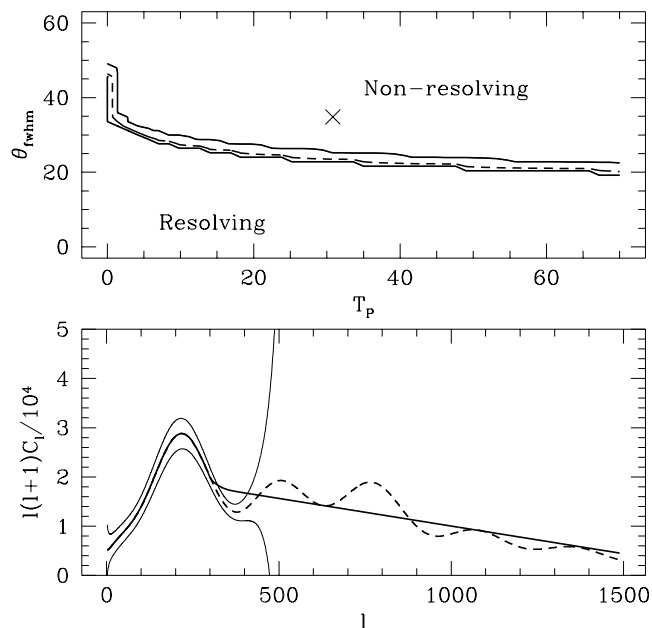


FIG. 5. A standard CDM curve is paired with a curve identical at low l and linear at high. The selected error bars are from an experiment which can clearly resolve the first peak, but which is unable to confirm the presence of secondary oscillations. Clearly the search for secondary peaks places high demands on satellite design even when the primary peak appears at larger angular scales.

satellite.

ACKNOWLEDGEMENTS: We thank P. Ferreira, J. Mageijo, D. Scott, and M. White for helpful conversations, and we thank M. White for allowing us to use his low Ω inflationary curves. The standard CDM curve is from N. Sugiyama [13]. We acknowledge support from PPARC (A.A.) and the Knowles Studentship of the University of London (B.D.W.).

REFERENCES

- [1] M. White, D. Scott and J. Silk, *Annu. Rev. Astron. Astrophys.* **32** 319-370 (1994).
- [2] A. Albrecht, D. Coulson and P. Ferreira, astro-ph/9505030, *Phys. Rev. Lett.* 1996 (In press)
- [3] J. Magueijo, A. Albrecht, D. Coulson and P. Ferreira, astro-ph/9511042, submitted to PRL.
- [4] R. Crittenden and N. Turok *Phys. Rev. Lett* **75** 2642 (1996).
- [5] W. Hu and M. White, “Acoustic Signatures in the Cosmic Microwave Background” astro-ph/9602019
- [6] L. Knox, *Phys. Rev. D* **52** 4307 (1995)
- [7] M. White and M. Srednicki, *Ap. J.* **443**, 6 (1995)
- [8] D. Scott, M. Srednicki and M. White, *Ap. J.* **421**, L5 (1994)
- [9] J. Magueijo and M. Hobson, “Cosmic Microwave Background experiments targeting cosmic strings Doppler peak signal”. MRAO-1900, DAMTP-96-13, Submitted to *PRL*.
- [10] M. Janssen *et al* “Direct imaging of the CMB from space” astro-ph/9602009 (1996).
- [11] E. Wright, G. Hinshaw, and C. Bennett, astro-ph/9510102 (1995)
- [12] M. Tegmark and G. Efstathiou, *An optimal method for subtraction foregrounds from multi-frequency CMB sky maps* MPI-PhT/95-62.
- [13] N. Sugiyama, *Ap.J.Supp.* **100** 281 (1995)